Electron transfer and ionization in proton-helium collisions studied using a Sturmian basis

Thomas G. Winter

Department of Physics, Pennsylvania State University, Wilkes-Barre Campus, Lehman, Pennsylvania 18627*
and Department of Physics, Rice University, Houston, Texas 77251

(Received 11 March 1991; revised manuscript received 3 May 1991)

Cross sections have been calculated for electron transfer into all states of hydrogen and for ionization in collisions between protons and helium atoms at proton energies from 50 to 200 keV. Cross sections for electron transfer into individual states up to $3d_2$, as well as the z component of the average electric dipole moment and of the cross product between the angular momentum and the Runge-Lenz vector for the $n=2$ and 3 levels, have also been determined. A coupled-state approach is taken using bases of about 50 Sturmian functions, extending earlier work on one-electron systems. The full two-electron interaction is included, neglecting, however, interatomic exchange. Detailed tests of convergence with respect to the size of basis have been carried out. It is found that the results for capture into all states and the individual states $1s$, $2s$, and $3s$, as well as the results for ionization, are converged to at least about 10%. There is excellent agreement with experimental results at least at the highest energy, where interatomic exchange is unimportant. Quantities involving p and d levels, on the other hand, are much more sensitive to the size of basis, and the agreement of the present and other coupled-state results with experimental results is less satisfactory.

PACS number(s): 34.70.+e, 34.50.Fa

I. INTRODUCTION

Electron transfer and ionization in collisions between protons and helium atoms are basic heavy-particle collision processes amenable both to experimental and theoretical study. At intermediate proton energies on the order of 100 keV the probability of either process is not small and so an accurate theoretical treatment would be expected to require the strong coupling of both channels.

The coupled-atomic-state treatment of electron transfer in proton-helium collisions dates back to 1965: Green, Stanley, and Chiang [1] reported a pioneering two-state calculation including the effects of interatomic exchange. (Including interatomic exchange means that the final-state wave function for the captured electron and the electron remaining behind is antisymmetrized.) In 1966, Bransden and Sin Fai Lam [2] also reported a two-state calculation, but neglecting exchange. They concluded that the sensitivity to the inclusion of interatomic exchange at higher energies, as well as to the choice of helium wave function, is small, on the order of 10% or less.

In 1967, Sin Fai Lam [3] reported a coupled-state calculation including also the $2s$ and $2p$ states of hydrogen. This calculation was extended in 1974 by Winter and C. C. Lin [4] to include the $3s$, $3p$, and $3d$ states of hydrogen. While both calculations provided individual excited-state cross sections to compare with experimental results, the inclusion of these excited states did not much affect the ground-state capture cross section at higher energies of several hundred kilo-electron-volts. A disagreement with experimental results therefore persisted for capture into all states and was attributed to the neglect of ionization channels [4]. (Winter and Lin also reported that they could not reproduce the $2s$ and $2p$ cross sections

of Sin Fai Lam using his smaller basis.)

Ionization channels were partly included for the first time in 1987 by Jain, C. D. Lin, and Fritsch [5] using an atomic basis augmented by pseudostates. (Unlike the previous calculations, theirs did not include the full two-electron potential.) However, Jain, Lin, and Fritsch did not report an ionization cross section which might have indicated the extent to which ionization channels were accurately represented, and they did not extend the calculations above 100 keV, where ionization channels would be expected to have a strong effect on electron transfer. Their primary intent was to compare with experimental off-diagonal elements of the $n=3$ density matrix then available below 100 keV. Finally, in 1990, Slim, Heck, Bransden, and Flower [6] enlarged the atomic-plus-pseudostate basis further to include 33 states and especially, for the first time since 1965, to include interatomic exchange as well. Their calculation confirmed the substantial effect of exchange at lower energies, while at their highest energy, 150 keV, the effect of exchange was generally found to be small.

The present coupled-state calculation is an extension of the calculation using a Sturmian basis previously carried out by Winter and co-workers for collisions of protons with He$^+$ (and other) ions [7–10]. This basis is potentially complete. The calculations systematically tested the convergence of cross sections with respect to basis size for the summed capture into all states, as well as ionization and capture into the ground state. It was concluded from these internal tests that the Sturmian cross sections for proton energies on the order of 100 keV are converged at least to within 10%. Agreement with experimental results confirms this. The present calculations will attempt to duplicate this success for He rather than He$^+$ targets. Furthermore, the calculation is more ambi-

tious than that for the one-electron system: Cross sections will be determined for capture into individual excited states, as well as quantities derived from off-diagonal elements of the density matrix. This will allow comparison with the wealth of experimental data which is lacking for the theoretically simpler but experimentally more difficult one-electron case.

The present calculation will be carried out for proton energies from 50 to 200 keV. At the lowest energy, electron transfer is the dominant channel, whereas at the highest energy, ionization is strongly dominant. This is also the energy range over which, according to the early results of Green, Stanley, and Chiang [1], and, to some extent, the very recent results of Slim et al. [6], interatomic exchange becomes less important; it will therefore be neglected in the present calculations. The present results and the results of Slim et al. will allow a determination of the relative sensitivity to exchange and basis size, including the sensitivity to ionization channels.

The outline of the paper is as follows. In Sec. II, the coupled-state method using Sturmian basis functions will be summarized. In Sec. III, numerical tests of the accuracy of matrix elements and cross sections will be described. In Sec. IV, tests of convergence with respect to basis size will be described. Finally, in Sec. V, cross sections and quantities obtained from off-diagonal elements of the density matrix will be presented and compared with experimental and other coupled-state results. Atomic units will be used unless otherwise indicated.

II. METHOD

The present coupled-state calculation is an extension of previous work by Winter and co-workers [7–10] on asymmetric one-electron systems such as p-He$^+$ using a Sturmian basis, following earlier work by Shakeshaft [11] and Gallaher and Wilets [12] on the symmetric p-H system. Recently, Winter studied direct excitation and ionization in MeV-energy proton-helium collisions using a coupled-state approach with a Sturmian basis [13]. Since only the direct (or He-centered) processes were of interest, the small electron-transfer channels at these high energies were neglected. The inclusion of these channels at the intermediate energies now being considered makes the present calculation a two-centered one, entailing the evaluation of velocity-dependent, charge-exchange matrix elements.

At the energies being considered here, the impact-parameter method will be used as in previous work. Extending the treatment of Shakeshaft [11] and Winter [7] to two-electron systems, the time-dependent electronic wave function is expanded in terms of approximate traveling atomic orbitals:

$$\Psi(\mathbf{r}_1,\mathbf{r}_2,t)=\sum_{k,\alpha,\beta} a_{k\alpha\beta}(t)f_{k\alpha\beta}(\mathbf{r}_1,\mathbf{r}_2,t) \ , \qquad (1a)$$

where

$$f_{k\alpha\beta}(\mathbf{r}_1,\mathbf{r}_2,t)=\psi_{k\alpha\beta}(\mathbf{r}_{1\alpha}(\mathbf{r}_1,t),\mathbf{r}_{2\beta}(\mathbf{r}_2,t))$$

$$\times \exp\left[-iE_{k\alpha\beta}t \mp \frac{i\mathbf{v}\cdot\mathbf{r}_1}{2}\right.$$

$$\left.\mp \frac{i\mathbf{v}\cdot\mathbf{r}_2}{2} - \frac{iv^2t}{4}\right] \ , \qquad (1b)$$

each $\psi_{k\alpha\beta}$ being an approximate atomic wave function or product of wave functions (to be described below) with corresponding approximate eigenvalue $E_{k\alpha\beta}$. Electron 1 is centered on nucleus α and electron 2 is centered on nucleus β (where α,β here denote $B=\mathrm{H}^+$ or $A=\mathrm{He}^{2+}$, unlike in Ref. [7]). The vectors $\mathbf{r}_{1\alpha}$ and $\mathbf{r}_1$, for example, are the positive vectors of electron 1 relative to the nucleus α and the midpoint of the internuclear line, and the upper or lower sign in the plane-wave factor $\exp(\mp i\mathbf{v}\cdot\mathbf{r}_1/2)$ is chosen according to whether $\alpha=A$ or B. The axis of quantization is chosen to be along the velocity $\mathbf{v}$ of B relative to A.

A. Sturmian basis

The approximate atomic wave functions $\psi_{k\alpha\beta}$ are obtained by diagonalizing the atomic Hamiltonians in finite Sturmian bases. If both electrons are bound to A, then one diagonalizes the Hamiltonian of helium

$$H_{AA}=-\tfrac{1}{2}\nabla_1^2-\tfrac{1}{2}\nabla_2^2-\frac{Z_A}{r_{1A}}-\frac{Z_A}{r_{2A}}+\frac{1}{r_{12}} \qquad (2)$$

($Z_A=2$ being the nuclear charge) in a finite two-electron basis $\varphi_{jAA}(\mathbf{r}_{1A},\mathbf{r}_{2A})$:

$$\langle \psi_{kAA}|H_{AA}|\psi_{k'AA}\rangle=E_{kAA}\delta_{kk'} \ , \qquad (3a)$$

$$\langle \psi_{kAA}|\psi_{k'AA}\rangle=\delta_{kk'} \ , \qquad (3b)$$

leading to the particular linear combinations

$$\psi_{kAA}=\sum_{j=1}^{j_{\max AA}} C_{kjAA}\varphi_{jAA} \ , \qquad (4)$$

where the two-electron basis functions φ_{jAA} will be described below. (Functions with double-letter subscripts are two-electron functions on one or possibly two centers; those with a single-letter subscript are one-electron functions. The function φ_{jAA} was denoted by Φ_j in Ref. [13].) If, on the other hand, electron 1 (the active electron) is bound to B and electron 2 to A, then one separately diagonalizes the one-electron Hamiltonians

$$H_B=-\tfrac{1}{2}\nabla_1^2-\frac{Z_B}{r_{1B}} \ , \quad H_A=-\tfrac{1}{2}\nabla_2^2-\frac{Z_A}{r_{2A}} \qquad (5)$$

in finite bases of Sturmian functions $\varphi_{jB}(\mathbf{r}_{1B})$, $\varphi_{jA}(\mathbf{r}_{2A})$; in summary,

$$\langle \psi_{k\gamma}|H_\gamma|\psi_{k'\gamma}\rangle=E_{k\gamma}\delta_{kk'} \ , \qquad (6a)$$

$$\langle \psi_{k\gamma}|\psi_{k'\gamma}\rangle=\delta_{kk'} \ , \qquad (6b)$$

where $\gamma=A,B$, leading to the particular linear combinations

$$\psi_{k\gamma} = \sum_{j=1}^{j_{\max\gamma}} C_{kj\gamma} \varphi_{j\gamma} , \quad \gamma = A, B . \tag{7}$$

The one-electron functions $\varphi_{j\gamma}$ with $j = nlm$ are Sturmian functions as described in Ref. [7]:

$$\varphi_{nlm\gamma}(\mathbf{r}_\gamma) = S_{nl\gamma}(r_\gamma) \mathcal{Y}_{lm}(\hat{\mathbf{r}}_\gamma) , \tag{8}$$

the $\mathcal{Y}_{lm}$ being modified (i.e., real) spherical harmonics. For the case $\alpha\beta = BA$, the full atomic wave function in Eq. (1b) is

$$\psi_{kBA}(\mathbf{r}_{1B}, \mathbf{r}_{2A}) = \psi_{kB}(\mathbf{r}_{1B}) \psi_{kA}(\mathbf{r}_{2A}) , \tag{9}$$

with energy $E_{kBA} = E_{kB} + E_{kA}$.

Only two kinds of terms will be retained in the sum over $\alpha\beta$ in Eq. (1): AA and BA terms as just described, AA terms representing the initial and other "direct" states centered on helium, and BA terms representing electron 1 captured (with electron 2 remaining behind). The terms AB and BB are neglected. The AB terms refer to electron 2 being captured (and 1 remaining behind); when combined with BA terms in a symmetric combination, they together represent interatomic exchange, which, as described in the Introduction, is being neglected at the energies of about 100 keV being considered here. The remaining BB terms refer to H^- states (states of double capture), which are neglected on the assumption that they are weakly populated and only slightly affect single capture or single ionization.

The helium basis functions $\varphi_{jAA}(\mathbf{r}_{1A}, \mathbf{r}_{2A})$ are as described in Ref. [13]: symmetrized products of Sturmian functions $\varphi_{nlmA}(\mathbf{r}_{1A})$ and $\varphi_{n'l'm'A}(\mathbf{r}_{2A})$. To keep the problem to a reasonable size, as in that paper, only ${}^1S$ and ${}^1P$ functions are included; ${}^1D$ and higher channels probably have only a small effect. (The dominant ionization channels at higher energies are of ${}^1P$ symmetry.) Extensive tables were presented in Ref. [13] indicating how the ${}^1S$ and ${}^1P$ energies vary as the Sturmian basis is enlarged.

B. Coupled equations

As in Ref. [7] for the one-electron case, the time-dependent electronic wave function, now given by Eq. (1), is substituted into the time-dependent Schrödinger equation, multiplied by the complex conjugate of one of the traveling atomic orbitals $f^*_{k\alpha\beta}$, and integrated over all space. One obtains a set of coupled differential equations for the expansion coefficients $a_{k\alpha\beta}$ [Eqs. (9)ff in Ref. [7], but with additional subscripts for the second electron].

If the electrons are assumed to be initially in the 1 ${}^1S$ state of helium labeled by $1AA$, then the initial condition for which the coupled equations are solved is

$$a_{k\alpha\beta}(-\infty) = \delta_{1AAk\alpha\beta} . \tag{10}$$

The probability of a transition to the kth state in which *either* electron is transferred is

$$P_{k,\text{trans}}(\rho) = 2|a_{kBA}(\rho, \infty)|^2 \tag{11}$$

at a given impact parameter ρ. The probability of ionization is

$$P_{\text{ioniz}}(\rho) = 2 \sum_{E_{kB}\,(>0)} |a_{kBA}(\rho, \infty)|^2 + \sum_{E_{kAA}\,(>-2)} |a_{kAA}(\rho, \infty)|^2 , \tag{12}$$

the sums being over states above the ionization thresholds of hydrogen and helium, representing charge transfer to the continuum and direct ionization, respectively.

As in previous work [4,7,13], the coupled equations are solved numerically using Hamming's method. Conservation of probability

$$\sum_{k,\alpha,\beta} |a_{k\alpha\beta}(\rho, \infty)|^2 = 1 \tag{13}$$

is here valid to 10^{-3}, usually 10^{-4}. The range of integration over $z = vt$ was typically taken to be from -30 to $+1000$, the upper limit allowing for long-range coupling between states on the same center.

The total cross sections $Q_{k,\text{trans}}$ and Q_{ioniz} for electron transfer and ionization are obtained by integrating the probabilities in Eqs. (11) and (12) over impact parameters:

$$Q = 2\pi \int_0^\infty d\rho\, \rho P(\rho) . \tag{14}$$

Simpson's rule has been used with the 12 points $\rho = 0(0.25)1$, $1(0.5)3$, and $3(1)6$, which is estimated to give a numerical accuracy of at least 1%. [The notation $\rho_0(\Delta\rho)\rho$ denotes points from ρ_0 to ρ with spacing $\Delta\rho$.]

C. Matrix elements

Many of the matrix elements in the coupled equations are expressible in terms of one-electron, one- and two-center integrals described in Refs. [7] and [13]. There are, in addition, two-electron matrix elements: first, the two-electron, two-center matrix elements $V_{12kBkAk'Bk'A}$ defined by

$$V_{12kBkAk'Bk'A}(\rho, z) = \left\langle \psi_{kB}(\mathbf{r}_{1B}) \psi_{kA}(\mathbf{r}_{2A}) \left| \frac{1}{r_{12}} \right| \psi_{k'B}(\mathbf{r}_{1B}) \psi_{k'A}(\mathbf{r}_{2A}) \right\rangle . \tag{15}$$

Although it may be possible to evaluate them analytically, it was decided to evaluate them numerically. The procedure is similar to that used to evaluate the velocity-dependent, two-electron charge-exchange integrals such as

$$V_{12n_1sAn_2sAj'Bj'A}(v, \rho, z) = \left\langle \varphi_{n_1sA}(\mathbf{r}_{1A}) \varphi_{n_2sA}(\mathbf{r}_{2A}) \left| \exp(i\mathbf{v}\cdot\mathbf{r}_1) \frac{1}{r_{12}} \right| \varphi_{j'B}(\mathbf{r}_{1B}) \varphi_{j'A}(\mathbf{r}_{2A}) \right\rangle \tag{16}$$

for $s^2\,{}^1S$ states of helium. This is evaluated by expanding $1/r_{12}$ as a power series in $r_</r_>$, where $r_<(r_>)$ is the lesser (greater) of r_{1A} and r_{2A}. The integral over r_{2A} then leads to the functions

$$_0f_{ns,n'l',l'}(Z_A,r_{1A})$$

$$= \int_0^\infty dr_{2A}\, r_{2A}^2 S_{ns}(Z_A,r_{2A})S_{n'l'}(Z_A,r_{2A})\frac{r_<^{l'}}{r_>^{l'+1}} \quad (17)$$

defined in Ref. [7] in the context of evaluating direct matrix elements, while the integral over $\hat{r}_{2A}$ can be done analytically. The remaining three-dimensional integral over $\mathbf{r}_1$ is evaluated in prolate spheroidal coordinates, as in the one-electron procedure in Ref. [7], using rotation matrices to transform the Sturmian functions into the molecular reference frame, although the integrand is now more complicated.

The integrals over the spheroidal coordinates λ and μ were evaluated numerically by 32-point Gauss-Laguerre and 40-point Gauss-Legendre quadratures, respectively. This evaluation of two-electron matrix elements for $s^2\,{}^1S$ states was carried out for 1,638 combinations of Sturmian functions at each required v and ρ (3×11 values) for 200 values of R (or $|z|$) ≤20 and 100 values between 20 and 40. The computer program to evaluate them was vectorized as fully as possible on Pennsylvania State University's IBM 3090-600S computer, the output for these and the other two-electron matrix elements occupying three 2400-ft magnetic tapes. (The total CPU time to calculate all two-electron matrix elements was about 60 h.) Five-point interpolation yielded values at the actual z encountered when integrating the coupled equations.

III. NUMERICAL TESTS

A. Matrix elements

The one-electron matrix elements have been evaluated using the same computer subroutines as were tested previously for calculations on one-electron systems [7]. Two-electron matrix elements now have also been checked extensively to guard against programming errors and numerical inaccuracy. These matrix elements are of four types: direct matrix elements and three different charge-exchange matrix elements, involving $(s^2)\,{}^1S$, $(p^2)\,{}^1S$, and ${}^1P$ "Sturmian" functions. For brevity, only the evaluation of the first type of charge-exchange matrix element is summarized in Sec. II C, and only tests for this type of matrix element will be described here. Similar tests were carried out for the other matrix elements.

First, numerous comparisons were made at a very small velocity ($v=10^{-4}$) with analytic values obtained independently [14] in the zero-velocity limit at one point $(\rho,R)=(2,3)$. Real parts of the matrix elements were compared for twelve combinations $n_1s_A n_2s_A n'l'm_B n'l'm_A \leq 2s^2 2p 2s$; eleven of these agree to eight digits, and the remaining one, to six digits. Imaginary parts for three combinations were also compared; these agree to eight digits too. Second, a comparison was also made with an analytic result obtained independently [14] to order v^2 for $1s$ states throughout;

there is eight-digit agreement up to a velocity 0.01 (whereas at this velocity there is only five-digit agreement with the zeroth-order result used in the first test). [A test was also carried out at the finite velocity $v=2$ in the $R\rightarrow0$ limit for one of the $(p^2)\,{}^1S$ matrix elements; there is eight-digit agreement with a simple expression obtained in this limit.]

Third, tests were made of the accuracy of these matrix elements with respect to the number of points in the numerical integrations over λ,μ by comparing values obtained with 24,40 and 32,96 points. These tests were carried out for a 59-state basis. Values were computed for $v=10^{-4}$, 1, 2, and $\sqrt{12}$; $R=0.25$, 1, 3, 20, and 40; and one value of ρ in each case. For $v\leq2$ ($E_p\leq100$ keV), most relative or absolute differences in the matrix elements are $\leq10^{-4}$ or 10^{-8}, respectively; the few exceptions occurred for very highly excited states. Although the larger differences encountered for $v=\sqrt{12}$ ($E_p=300$ keV) were probably tolerable, the final calculations were confined to energies $E_p\leq200$ keV, using 32-point integration over λ at all energies.

B. Coupled equations

The sensitivity to various parameters in integrating the coupled equations has been tested by varying these parameters from those chosen, much as in previous work [7–10]. Charge-exchange coupling was neglected beyond $R=40$ rather than the usual 30, the range of integration over z was extended considerably beyond the typically chosen range from -30 to $+1000$, and the truncation-error limits were made 10 times more stringent than usual. These tests were carried out with a 39-state basis at $\rho=0.25$, $E_p=100$ keV (as well as with a five-state basis at $\rho=1$). The sensitivity of probabilities for capture into individual states $nl\leq3d$ is at most 1%.

C. Cross sections

As an overall test of the two-electron, Sturmian computation, cross sections have been calculated deleting all but five atomic states and all but eleven atomic states after diagonalizing the atomic Hamiltonians. These cross sections were then compared with the corresponding atomic-state results of Winter and Lin [4]. The five atomic states are the ground state of helium and the $1s$, $2s$, and $2p_{0,1}$ states of hydrogen (with the He$^+$ ion in the ground state); the eleven atomic states include also the $3s$, $3p_{0,1}$, and $3d_{0,1,2}$ states of hydrogen. In the present Sturmian calculation, the five-atomic-state basis was formed from 23 functions: twelve $(s^2)\,{}^1S$ functions representing the He ground state, nine s functions representing the H $1s,2s$ states, plus H $2p_{0,1}$ functions (which are identical to atomic-state functions); the eleven-atomic-state basis was formed from 37 functions: seven $(s^2)\,{}^1S$ functions representing the He ground state, thirteen s functions and fourteen p functions representing H $1s$, $2s$, $3s$, $2p_{0,1}$, and $3p_{0,1}$ states, plus $3d_{0,1,2}$ functions. The cross sections were calculated at a proton energy of 100 keV. The present five-state and eleven-state cross sections for capture into the individual $1s$, $2s$, and $2p$ states agree with

those of Winter and Lin to within 7%. For capture into the 3s, 3p, and 3d states, the present eleven-state cross sections agree with those of Winter and Lin to within 12%, and it is estimated that this agreement would be improved to better than 10% if additional Sturmian functions were used to represent the 3s state. The overall agreement of better than 10% with the atomic-state results of Winter and Lin is within the slight uncertainty due to different representations of the He(1 ^1S) wave function.

As noted in the Introduction, Winter and Lin pointed out substantial differences between their five-atomic-state 2s,2p cross sections and the corresponding five-atomic-state cross sections of Sin Fai Lam [3] over a wide range of energies. The coupled-atomic-state results of Sin Fai Lam, unlike those of Winter and Lin, also fail to tie in to the first-order Born cross sections at the high energy of 1 MeV. In view of this and the agreement between the present cross sections and those of Winter and Lin, the cross sections of Sin Fai Lam appear to be in error.

IV. TESTS OF THE SIZE OF BASIS

Numerous tests have been performed of the sensitivity of the results to the size of the Sturmian basis. Unlike tests in previous one-electron studies [7–10], the sensitivity for capture into each excited state (up to 3d), as well as ionization, was monitored. These tests were carried out at two important impact parameters $\rho=0.25$ and 1.5 for the intermediate proton energy of 100 keV. The probability times impact parameter $\rho P(\rho)$ for electron transfer into the 3s and 3p states, and for ionization, peaks at impact parameters in the range 1–1.5 for most bases. For capture into lower-lying states, $\rho P(\rho)$ peaks at smaller impact parameters $\rho \simeq 0.75$, and $\rho P_{3d}(\rho)$ peaks at still smaller ρ. On the other hand, the probability itself, without the ρ weighting used to obtain the integrated cross section, peaks at the smallest calculated impact parameter $\rho=0.25$ for all states with almost all bases.

The sensitivity to functions centered on the proton is different from the sensitivity to functions centered on the helium nucleus. These sensitivities will be considered separately in Secs. IV A and IV B.

A. Sensitivity to proton-centered functions

Consider first the sensitivity to s Sturmian functions centered on the proton. Calculations have been carried out for a sufficient (fixed) number of other functions to give qualitatively correct overall character [15]. Shown in Fig. 1 is the probability times impact parameter $\rho P(\rho)$ versus the number of s Sturmian functions $n_{s\text{ max}}$ at the impact parameter $\rho=1.5$. It is seen that the *percent* sensitivity is generally greater for channels of lower probability, and that with the possible exceptions of the $n=3$ levels, particularly 3d, all probabilities appear to be stabilizing by $n_{s\text{ max}} \simeq 7$. The 3d probability does not appear stable even for $n_{s\text{ max}} \simeq 13$ at this impact parameter. However, $\rho P_{3d}(\rho)$ peaks at a much smaller value of ρ, and the variation of $\rho P_{3d}(\rho)$ with $n_{s\text{ max}}$ can be seen in Fig. 1 to be much less at $\rho=0.25$ than at 1.5. The value
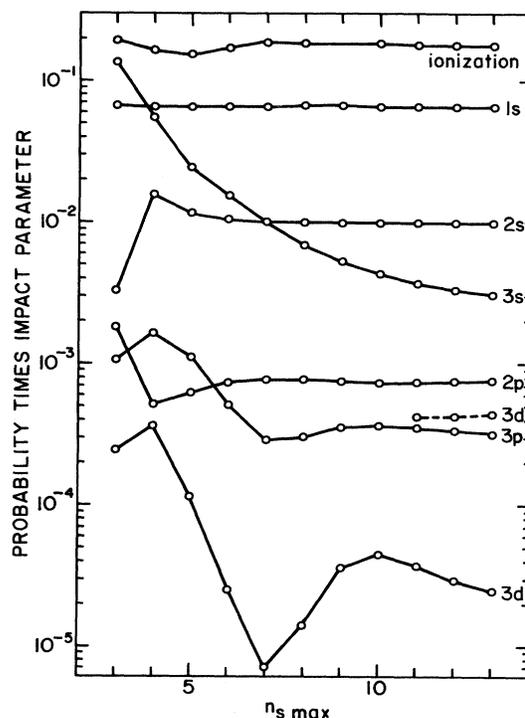

FIG. 1. Probability times impact parameter $\rho P(\rho)$ vs the number of s Sturmian functions, $n_{s\text{ max}}$, centered on the proton for ionization and for electron transfer into the states 1s to 3d in 100-keV, p-He collisions. Solid curves, $\rho=1.5$; dashed curve, $\rho=0.25$.

of $\rho P_{3s}(\rho)$ varies significantly for $n_{s\text{ max}} > 7$ due to the difficulty of representing the 3s atomic state with Sturmian functions; however, the behavior is monotonic and predictable, and the infinite s-basis limit is estimated to be only 10% below the value for $n_{s\text{ max}}=13$. Not shown in Fig. 1 are variations at $\rho=0.25$ for states other than 3d; these variations are similar to those at $\rho=1.5$.

Consider second the sensitivity to p Sturmian functions centered on the proton. Shown in Fig. 2 is the probability-times-impact parameter versus the maximum quantum number $n_{p\text{ max}}$ of the p Sturmian functions [16]. Except for ionization, only values at the impact parameter $\rho=1.5$ are shown; values of the smaller impact parameter $\rho=0.25$ have comparable or somewhat smaller variations. It is seen that the dependence on p functions is somewhat similar to that on s functions in that the smaller probabilities generally display the larger percent variations. With the exception of ionization, all values for $\rho=1.5$ are fairly stable by $n_{p\text{ max}} \simeq 5$. Values for ionization are also shown at the smaller impact parameter since the behavior there is different: At $\rho=0.25$, there is little sensitivity, whereas at $\rho=1.5$, the probability is just beginning to turn over, and perhaps stabilize, at the largest value of $n_{p\text{ max}}$. This is likely due to the representation of ionization at 100 keV by only s functions centered
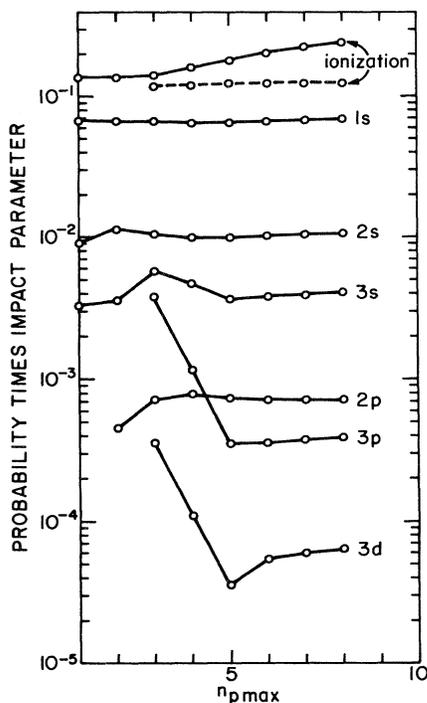
FIG. 2. Probability times impact parameter $\rho P(\rho)$ vs the maximum quantum number $n_{p\ max}$ of p Sturmian functions centered on the proton for ionization and for electron transfer into the states $1s$ to $3d$ in 100-keV, proton-He collisions. Solid curves, $\rho=1.5$; dashed curve, $\rho=0.25$. The notation $n_{p\ max}=1$ refers to the omission of all p functions centered on the proton.

FIG. 3. Probability times impact parameter $\rho P(\rho)$ vs the number of $n_1 s n_2 s\ ^1S$ Sturmian functions (formed from one-electron $n_1 s, n_2 s$ Sturmian functions) centered on the He nucleus for ionization and for electron transfer into the states $1s$ to $3d$ in 100-keV, p-He collisions. Solid curves, $\rho=1.5$; dashed curves, $\rho=0.25$. The smallest He-centered bases has $n_1 \leq 2$, $n_2 \leq 4$; for the larger bases, $n_1 \leq 3$, $n_2 \leq 5(1)9$, the two states of highest energy centered on the He nucleus are omitted, and, in addition, the state of highest energy centered on the proton is omitted after diagonalizing the atomic Hamiltonians. In all cases, $n_1 \leq n_2$.

on He and s and p functions centered on the proton. At high energies, ionization is dominated by p channels centered on He and it is difficult to represent these channels at larger impact parameters with a small number of p functions centered on the other nucleus.

A combined test of the sensitivity to both s and p Sturmian functions centered on the proton has been carried out at the highest proton energy being considered, 200 keV: Cross sections to be presented in Sec. V have been calculated using bases of 41 and 46 states. The 46-state basis is the 41-state basis augmented by $12s$, $13s$, $7p_{0,1}$, and $8p_{0,1}$ Sturmian functions centered on the proton (except that the negligible highest s state has been removed after diagonalizing the Hamiltonian of hydrogen). The 41- and 46-state cross sections for capture into the individual $1s$, $2s$, $2p$, and $3p$ states differ by at most 5%, while for $3s$ and $3d$ the differences are 10% and 25%, respectively.

B. Sensitivity to helium-centered functions

Consider first the sensitivity at 100 keV to $s^2\ ^1S$ functions, shown in Fig. 3 for both impact parameters $\rho=0.25$ and 1.5, except that for $\rho=0.25$ the values for $1s$, $2p$, and $3d$ are omitted. It is seen that the variation with respect to the number of He-centered functions [17] is larger for the smaller probabilities, as was also noted
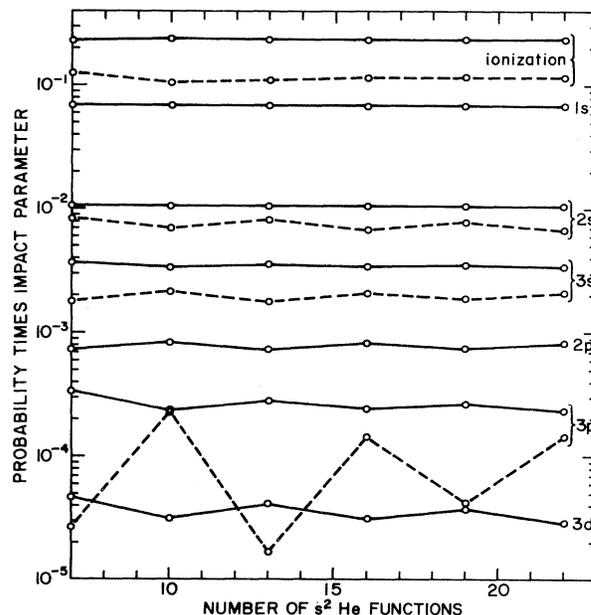
generally to be the case for the variation with respect to proton-centered states. For ionization and capture into the ground state, the variation is insignificant. (The ground-state values omitted at $\rho=0.25$ are very close to those at $\rho=1.5$.) For capture into excited states, however, the variation is much larger at the smaller impact parameter than at the larger one, unlike the variations with respect to proton-centered states. For the $2s$ and $3s$ states, the capture probability displays a small but persistent oscillation at the smaller impact parameter as the basis is enlarged. For the $2p$, $3p$, and $3d$ states, there are noticeable oscillations at the larger impact parameter which become very large at the smaller impact parameter. (The oscillations for $2p$ and $3d$, not shown at $\rho=0.25$, are similar to those for $3p$.) These oscillations are attributable to the strong effect of ionization channels, here of s type, on the small capture probabilities. This effect is pronounced at the smaller impact parameter, where there is greater overlap between proton- and He-centered states. The convergence with respect to the He-centered basis is very slow. From the "perspective" of the proton-centered states, the He-centered functions

form a slowly convergent series, since each such function contains a factor $e^{-i\mathbf{v}\cdot\mathbf{r}}$ which is significantly oscillatory at 100 keV ($v=2$). (A Sturmian basis forms a complete set; a Sturmian basis multiplied by $e^{-i\mathbf{v}\cdot\mathbf{r}}$ is also complete, but more slowly convergent.)

The overall sensitivity at 100 keV to $s^2\,{}^1S$ He functions may be summarized by comparing cross sections integrated over impact parameter for the two-largest bases—48- and 51-state bases—used in the preceding test at two impact parameters. These cross sections, which will be presented in Sec. V, indicate a range of sensitivity; the larger-basis one is not necessarily to be preferred. For the two largest cross sections—those for ionization and electron transfer to the ground state—the 48- and 51-state cross sections differ by at most 0.3%; for transfer into the 2s or 3s states, they differ by at most 4%; and for transfer into the 2p or 3p states, by at most 11%. In the case of 2p or 3p states, this fairly small integrated difference is in spite of the sensitivity at small impact parameters $\rho\simeq0.25$. However, for the 3d cross section, which receives its greatest contribution from these impact parameters, the 48- and 51-state values differ by a factor of two.

Consider second the sensitivity to $1snp\,{}^1P$ functions, shown in Fig. 4, at the larger impact parameter $\rho=1.5$
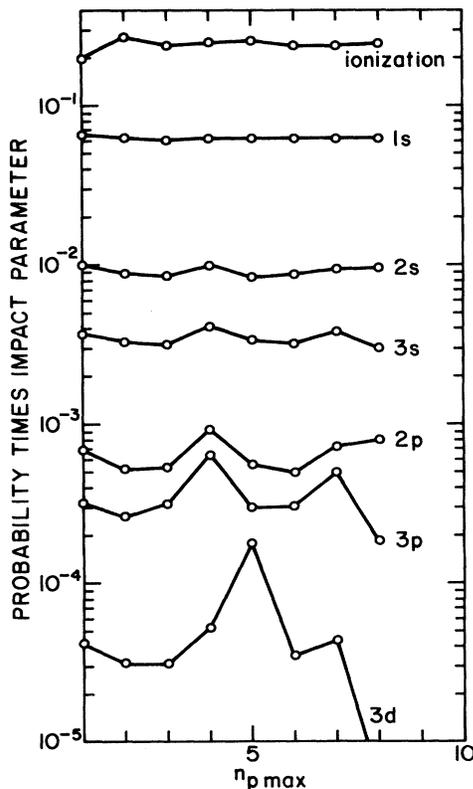
only [18]. It is seen that the sensitivity to ${}^1P$ functions at $\rho=1.5$ is greater than the previously noted sensitivity to $s^2\,{}^1S$ functions at this impact parameter and, indeed, is comparable to that at $\rho=0.25$ for ${}^1S$ functions. This sensitivity to p functions centered on the helium nucleus has been explored further by considering the simpler one-electron system in which the target is a He^+ ion rather than a helium atom. Basis convergence for this one-electron system was studied previously [7–10] in detail for ionization and ground-state (as well as all-state) capture, but not for capture into individual excited states. The variations with respect to p functions are shown in Fig. 5 for the one-electron case [19]. These variations are seen to be significant for the one-electron case as well.

Not shown are variations with respect to the same one-electron basis, but for a target nucleus of charge $Z_A=1.6875$ rather than 2, corresponding more closely to the two-electron problem with the active electron initially in the ground state of helium. These variations are similar except that the oscillations occur for larger values of $n_{p\,\max}$ due to the longer range of Sturmian functions for the smaller value of Z_A. Further insight can be obtained by plotting the variations with respect to basis size on a nonlogarithmic scale, and for a larger range of bases, up to $n_{p\,\max}=14$. This is accomplished by first subtracting from each probability its value for one particular basis (that for which $n_{p\,\max}=12$). Shown in Fig. 6 are these normalized probabilities for capture into all (available) states, for ionization, and for the sum of these two probabilities. It is seen that as the basis is enlarged [20], the
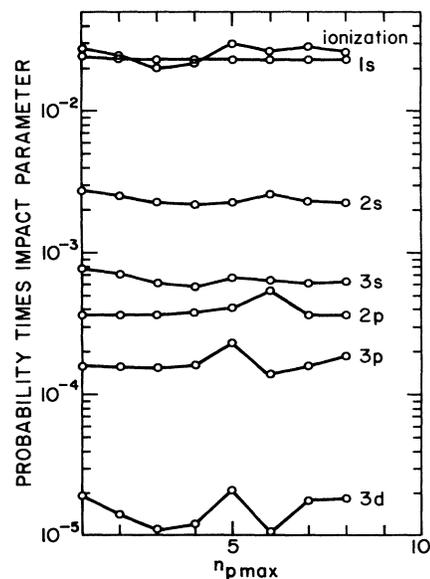

FIG. 4. Probability times impact parameter $\rho P(\rho)$ vs the maximum quantum number $n_{p\,\max}$, for $1snp\,{}^1P$ functions centered on the He nucleus for ionization and for electron transfer into the states $1s$ to $3d$ in 100-keV, proton-He collisions. Solid curves, $\rho=1.5$. The notation $n_{p\,\max}=1$ refers to the omission of all p functions centered on the He nucleus.

FIG. 5. Probability times impact parameter $\rho P(\rho)$ vs the maximum quantum number $n_{p\,\max}$ of p Sturmians centered on the He^+ nucleus for ionization and for electron transfer into the states $1s$ to $3d$ in 100-keV, proton-He^+ collisions. Solid curves, $\rho=1.5$. The notation $n_{p\,\max}=1$ refers to the omission of all p Sturmians centered on the He^+ nucleus.
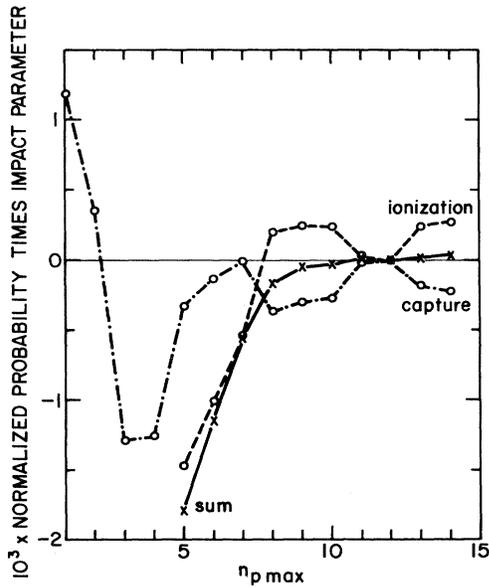
FIG. 6. Normalized probability times impact parameter $\rho P(\rho)$ vs the maximum quantum number $n_{p\,\text{max}}$ of p Sturmians centered on the He^+ nucleus for ionization (dashed curve) and electron transfer into all available states (dash-dotted curve) in 100-keV, proton-He^+ collisions at $\rho = 1.5$. The ionization curve includes also excitation of all other available He^+ states with $n \geq 4$. The solid curve is the sum of the other two curves. The He nucleus is assumed to have a charge $Z_A = 1.6875$.

capture and ionization probabilities oscillate out of phase and probability shifts back and forth between the two, the sum remaining relatively constant. This amplifies and reinforces what was stated previously for s-type, target-centered functions: that target-centered functions form a slowly convergent series as far as capture is concerned. By contrast, the effect of target-centered functions on the direct excitation of *target*-centered states damps out quickly as the basis is enlarged (not shown in Fig. 6).

The ionization channels at 100 keV are apparently well described even without $1snp$ ^1P functions, in view of the agreement with experimental results to be described in Sec. V. Considering the persistent sensitivity of capture channels to these functions even for large bases, it has been decided to omit the $1snp$ ^1P functions entirely at 100 keV. On the other hand, this is not possible at 200 keV; there, the $1snp$ ^1P functions will be seen in Sec. V to be necessary to represent ionization. The presumably significant sensitivity of capture channels to the inclusion of these functions is estimated by comparing cross sections with and without these functions: Differences are 11–15 % for the $1s$, $2s$, and $3s$ states, a factor of 2 for the $2p$ and $3p$ states, and 34% for the $3d$ states. (The basis omitting the $1snp$ ^1P functions includes 48 functions: 19 n_1sn_2s ^1S functions centered on helium and 29 functions centered on the proton. The other basis includes 46 functions: ten $1snp_{0,1}$ ^1P functions with $n \leq 6$, only seven

n_1sn_2s ^1S functions, and the 29 proton-centered functions included in the 48-state basis. The comparison is thus a composite test of the sensitivity to ^1P and ^1S functions.) Although the 46-state basis contains ^1P ionization channels necessary to obtain an ionization cross section, while the 48-state basis does not, it is not clear, in the absence of additional convergence studies, whether the $2p$, $3p$, and $3d$ cross sections obtained with the 46-state basis at 200 keV are superior to those obtained with the 48-state basis.

Finally, consider the sensitivity to p^2 ^1S functions centered on the helium nucleus. As described in Ref. [13], these functions account for most of the angular correlation in the ground state of helium. Convergence tests have been carried out at the same proton energy (100 keV) and impact parameter (1.5) as in previously described tests in the present paper. The effect of p^2 functions is found to be smaller than the effect of the other functions previously considered: the functions $2p^2$, $2p3p$, and $3p^2$ affect the $1s$, $2s$, $3s$, and $2p$ probabilities by at most 3%, while the effects on the $3p$ and $3d$ probabilities are 9% and 23%, respectively; the additional functions $2p4p$, $3p4p$, and $4p^2$ have a reduced effect, 2% and 16%, on the $3p$ and $3d$ probabilities, respectively [21]. These p^2 ^1S functions are probably not very important at any of the energies considered, and have been omitted.

V. COMPARISON WITH EXPERIMENTAL AND OTHER COUPLED-STATE RESULTS

Cross sections for electron transfer into states of a given angular momentum l show greater similarity than those for a given principal quantum number n. They will therefore be presented by l, starting with the largest, s-state cross sections and the ionization cross section, which is also large. The small, sensitive cross sections and off-diagonal quantities for the magnetic sublevels will be presented last.

A. Ionization and capture into all states and the 2s and 3s states

Sturmian cross sections for ionization and capture into all states and the $2s$ and $3s$ states are shown in Fig. 7 along with experimental and other coupled-state results. (These Sturmian cross sections, as well as those for capture into the $2p$, $3p$, and $3d$ states, are also given in Table I.) Cross sections for capture into all states are shown, rather than for capture into the $1s$ state, in order to compare with available experimental results.

Consider first that cross section which is the largest over most of the energy range being considered here: the ionization cross section, which exceeds the cross section for capture into all states for proton energies above 65 keV, and which may be expected to have some effect on the capture cross section over the full energy range of interest, 50–200 keV, and, indeed, a large effect at the highest energy. The experimental ionization cross section of Shah and Gilbody [22] shown in Fig. 7 has an overall estimated error of 9–10 % within the energy range of overlap, 64–200 keV, with the present study.

[The present calculation takes limited account of double as well as single ionization. However, the experimental single-plus-double-ionization cross section [22] (not shown in Fig. 7) is at most 1% larger than the single-ionization cross section.] Estimating the Sturmian cross section at 64 keV (not shown), there is seen to be agreement with the experimental results within the estimated experimental error over the full overlapping energy range. Thus the flux into ionization channels is accounted for in the present study. Although two of the other coupled-state calculations [5,6] include some pseudo-states representing ionization, ionization cross sections were not reported.
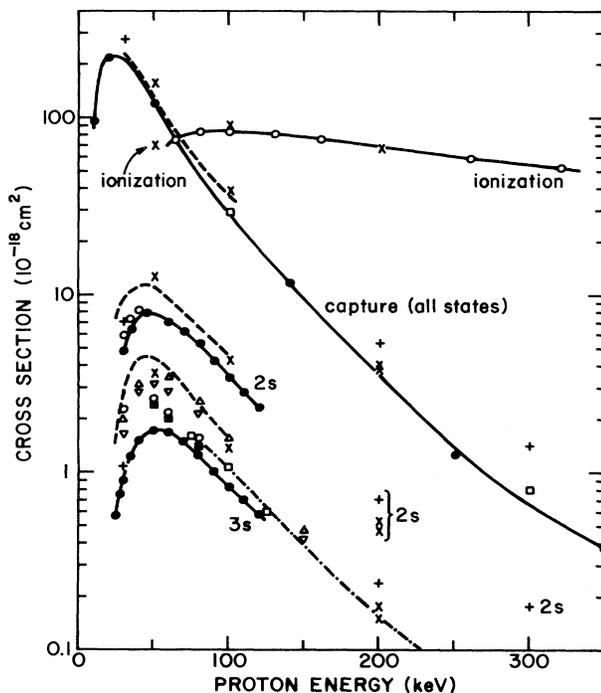
Consider second the cross sections for electron transfer

FIG. 7. Cross sections for ionization, capture into all states, and capture into the 2s and 3s states in collisions between protons and helium atoms. Coupled-state results: crosses, present 46–51-Sturmian (40-Sturmian at 50 keV); plus signs, 11-atomic-state, Winter and Lin (Ref. [4]); dashed curves, 19-state augmented atomic orbital (AO+), Jain, Lin, and Fritsch (Ref. [5]); erect and inverted triangles, 33-psuedostate without and with exchange, respectively, Slim et al. (Ref. [6]). The experimental results are represented as follows. Ionization: open circles and solid curve, Shah and Gilbody (Ref. [22]). Capture into all states: solid circles and solid curve, Barnett and Reynolds (Ref. [24]); open squares, Toburen, Nakai, and Langley (Ref. [25]). Capture into the 2s state: solid circles and solid curve, Hughes et al. (Ref. [27]); open circles, Andreev, Ankudinov, and Bobashev (Ref. [29]). Capture into the 3s state: solid circles and solid curve, Hughes et al. (Ref. [28]); open squares and dash-dotted curve, Conrads et al. (Ref. [26]); open circles, Lenormand (Ref. [30]); solid squares, Brower and Pipkin (Ref. [31]). Some overlapping results have been omitted.

into all states. The excited-state contribution to the Sturmian capture cross section [23] increases from 19% at 50 keV to 26% at 100 keV to about 35% at 200 keV, whereas the high-energy Born estimate from an n^3 rule is 20%. The experimental cross sections of Barnett and Reynolds [24] and Toburen, Nakai, and Langley [25] have estimated total errors of up to 15% and 10%, respectively. There is agreement between the present results and the experimental results at the highest energy, 200 keV, of the Sturmian calculation. On the other hand, the coupled-atomic-state results of Winter and Lin [4] are seen to be substantially too high at 200 and 300 keV; the same is true of earlier coupled-atomic-state results [1,2]. Thus a long-standing disagreement at high energies between coupled-state theory and experiment has been removed, apparently by the inclusion of ionization channels. At the lower energies ($E_p \lesssim 100$ keV), the Sturmian results are similar to the coupled-state results of Winter and Lin and exceed the experimental results—by about 25% in the present case. Thus the effect of ionization channels does not appear to be a factor here. Rather, it may be the effect of interatomic exchange [1], neglected in both calculations. Its inclusion would probably lower the cross sections by about 10% at these lower energies, bringing the theoretical results just about within the uncertainty 10–15% of the experimental cross sections. The coupled-state results of Jain, Lin, and Fritsch [5] in a one-electron model lie between the present coupled-state results and the experimental results in the energy range 50–100 keV.

Consider now the cross sections for capture into the 2s and 3s states. The energy dependence of these cross sections is seen in Fig. 7 to be similar to that for capture into all states. The relations among theoretical and experimental results are also similar to those for total capture: At energies of at least 200 keV, the coupled-atomic-state cross section of Winter and Lin [4] substantially exceeds the experimental result of Conrads, Nichols, Ford, and Thomas [26] for the 3s states, whereas the 48- and 46-state Sturmian values at 200 keV bracket the experimental curve. There are no 2s experimental results with which to compare at these high energies; however, the coupled-atomic-state result of Winter and Lin again lies above the coupled Sturmian results. In all these cases— total capture and capture into the 2s and 3s states—the inclusion of ionization channels thus appears necessary at energies of at least 200 keV. The situation for the 2s and 3s states at lower energies is qualitatively similar to that for total capture: The present Sturmian results and the atomic-state results of Winter and Lin lie above the results of Hughes et al. [27,28] by 20% to up to a factor of 2 for the 2s and 3s states. Part of this discrepancy may be experimental: The 2s result of Andreev, Ankudinov, and Bobashev [29] and the 3s results of Conrads et al. [26], Lenormand [30], and Brower and Pipkin [31] lie above those of Hughes et al. Nevertheless, some of the discrepancy is probably due to the neglect of interatomic exchange in the present calculation and that of Winter and Lin: the results of Slim et al. [6] with and without exchange show that for 3s the inclusion of exchange would lower the cross section by 15% and bring it closer

TABLE I. Sturmian cross sections (in units of 10^{-18} cm^2) for electron transfer into the individual states $nl \leq 3d$, all available states, and ionization in collisions between protons and ground-state helium atoms.

Proton energy (keV)	No. of basis functions	State							
		1s	2s	3s	2p	3p	3d	All	Ioniz.
50	40[a]	133	12.5	3.59	2.29	1.18	0.143	158	70.0
100	37[b]	30.1	4.56	1.38	0.667	0.172	0.048	38.8	91.9
100	48[c]	30.2	4.34	1.34	0.520	0.165	0.013	38.2	89.9
100	51[d]	30.3	4.19	1.36	0.483	0.185	0.028	38.3	90.0
200	48[c]	3.07	0.464	0.150	0.070	0.026	0.0046	3.98	38.5
200	41[e]	2.74	0.532	0.193	0.128	0.054	0.0083	3.92	66.4
200	46[f]	2.74	0.522	0.175	0.127	0.052	0.0065	3.82	67.4

[a]The 15 $n_1 s n_2 s$ ^1S functions centered on the He nucleus with $n_1 \leq 3$, $n_1 \leq n_2 \leq 6$ (the four highest states being dropped after diagonalizing the He Hamiltonian) and the 30 Sturmian functions centered on the proton up to 13s, $8p_{0,1}$, and $3d_{0,1,2}$ (with the highest s state being dropped after diagonalizing the H Hamiltonian, and the He$^+$ ion assumed to be in the ground state). To avoid linear dependence for $\rho \leq 0.5$, the contribution there was estimated using a basis with four fewer ^1S functions.

[b]The seven $n_1 s n_2 s$ ^1S functions centered on the He nucleus with $n_1 \leq 2$, $n_1 \leq n_2 \leq 4$ and the 30 Sturmian functions centered on the proton up to 13s, $8p_{0,1}$, and $3d_{0,1,2}$.

[c]The 21 $n_1 s n_2 s$ ^1S functions centered on the He nucleus with $n_1 \leq 3$, $n_1 \leq n_2 \leq 8$ (the two highest states being dropped after diagonalizing the He Hamiltonian), plus the proton-centered states in footnote a.

[d]The basis as in footnote c, but for $n_2 \leq 9$, i.e., three additional ^1S functions.

[e]The He-centered functions as in footnote b and the proton-centered Sturmian functions up to 11s, $6p_{0,1}$, and $3d_{0,1,2}$, plus the ten additional functions $1snp_{0,1}$ ^1P, $n \leq 6$ centered on the He nucleus.

[f]The basis as in footnote e plus the 12s, 13s, $7p_{0,1}$, and $8p_{0,1}$ Sturmian functions centered on the proton (with the highest s state dropped after diagonalizing the H Hamiltonian), i.e., the proton-centered functions as in footnote a.

to experiment. The differences among the coupled-state results without exchange are at most 14% for the 2s and 3s state at 50–100 keV (except for a 20% difference with the result of Jain, Lin, and Fritsch for the 3s state at 50 keV).

B. Capture into the 2p and 3p states

Sturmian cross sections for electron transfer into the 2p and 3p states are shown in Fig. 8 along with experimental and other coupled-state results. (The Sturmian cross sections are also given in Table I.) The 2p and 3p cross sections have a similar energy dependence and, particularly at higher energies, are smaller than the corresponding s-state cross sections.

Consider first the cross sections at the highest energy of the present calculations, 200 keV. It is seen that the 48- and 46-state Sturmian results bracket the experimental curve of Ford and Thomas [32], as well as the 11-atomic-state result of Winter and Lin [4]. As discussed in Sec. IV B, the difference between the 48- and 46-state Sturmian results reflects the sensitivity to ionization channels at high energies, which is considerably greater for p states than for s states. The Sturmian results at 200 keV also bracket the 11-atomic-state result for the 2p state. There are no experimental results for the 2p state at this high energy. The experimental results of Hughes et al. [27], stopping at 140 keV, would appear to extrapolate to the high side of the Sturmian results at 200 keV. For either state at this energy, the neglect of interatomic exchange in the present calculations is probably valid:
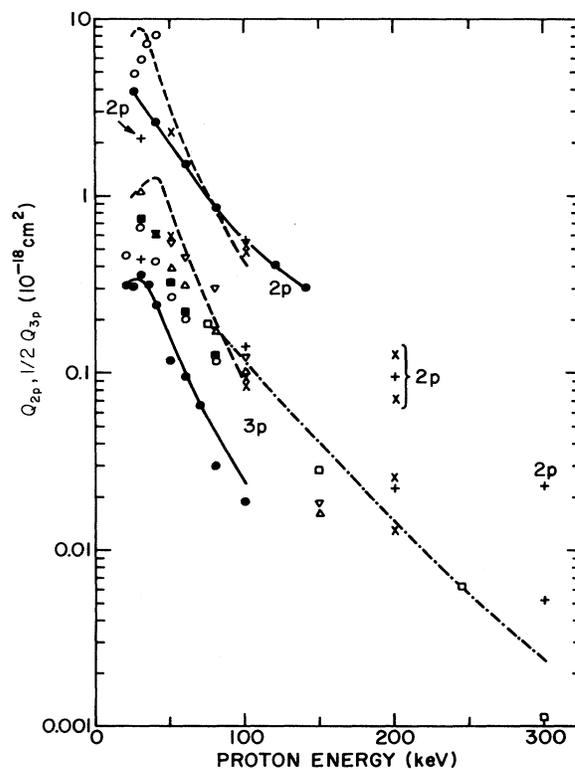

FIG. 8. Cross sections for capture into the 2p state and cross sections divided by two for capture into the 3p state in collisions between protons and helium atoms. The notation is as in Fig. 7, except that the open squares and dash-dotted curve refer to the experimental results of Ford and Thomas (Ref. [32]) for 3p.

Even at the lower energy of 150 keV, the $3p$ results of Slim et al. [6] with and without exchange differ by only 14%.

Consider now the cross sections at lower energies 50–100 keV. It is seen that the Sturmian cross section for the $2p$ state is within 15% of the experimental curve of Hughes et al. [27]. However, the early low-energy data of de Heer, van Eck, and Kistemaker [33] (not shown) and Andreev, Ankudinov, and Bobashev [29] for this state are considerably higher. The effect of exchange would probably be to *raise* the p Sturmian cross sections at these energies: the $3p$ cross section of Slim et al. [6] with exchange is 33% above that without exchange at 50 keV and 21% above it at 100 keV; this effect is opposite in sign to and larger than the effect for s states previously noted. If corrected for exchange in this way, the $3p$ Sturmian cross sections tie in with the experimental result of Ford and Thomas [32] at 100 keV and may also agree with the experimental results of Lenormand [30] and Brower and Pipkin [31] extrapolated from 80 to 100 keV. (The $3p$ experimental curve of Hughes et al. [28] is considerably below the other experimental results in the energy range 80–100 keV; this difference has been discussed previously [32].) Correcting the $3p$ results for exchange at 50 keV would appear to place the present results substantially above experimental results at this energy. However, there is a considerable basis sensitivity here: the present coupled-state results and those of Jain, Lin, and Fritsch [5] and Slim et al. [6] without exchange differ by up to a factor of 2, the present results lying between those of Refs. [5] and [6]; there is much closer agreement (within 20%) at 100 keV.

C. Capture into the $3d$ state

Sturmian cross sections for electron transfer into the $3d$ state are shown in Fig. 9 along with the experimental and other coupled-state results. (The Sturmian cross sections are also given in Table I.) The $3d$ cross section is comparable in magnitude to the $3p$ cross section at lower energies, but most of the results shown in the figure indicate that it decreases more rapidly with energy than the $3p$ cross section and is significantly smaller at higher energies. Surprisingly, unlike for the $3p$ state, the effect of interatomic exchange appears to be small: the results of Slim et al. [6] with and without exchange differ by at most 8%, at least above 30 keV; only the results with exchange are therefore shown. At the highest energy of the present calculation, 200 keV, the difference between the 48- and 46-state Sturmian results is significant, as was seen previously for the $3p$ state, the difference representing sensitivity to ionization channels. The experimental results of Ford and Thomas [32] show a surprising rise between 150 and 250 keV, but the data are sparse; the experimental results of Hughes et al. [28] are only reported for energies up to 100 keV. One can only report rough agreement between theory and experiment at 200 keV.

Consider the $3d$ results of lower energies from 50 to 100 keV. At 100 keV, as discussed in Sec. IV B, there is a factor-of-2 difference in the 48- and 51-state Sturmian results due to the sensitivity to ionization channels. The coupled-state results of Jain, Lin, and Fritsch [5] and
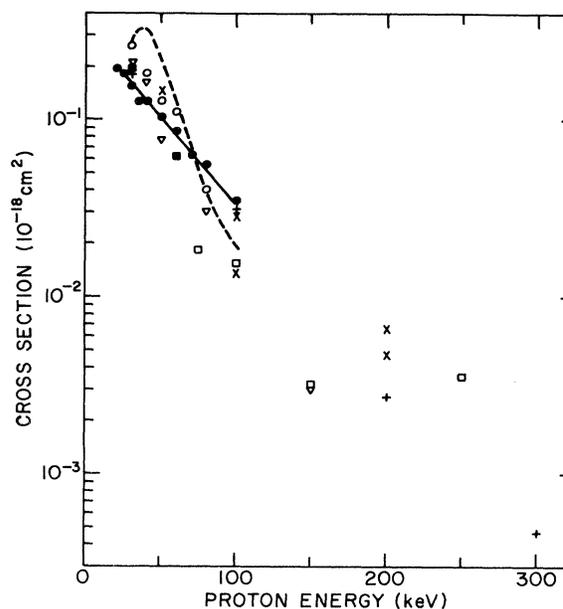
FIG. 9. Cross sections for capture into the $3d$ state in collisions between protons and helium atoms. The notation is as in Fig. 8.

Slim et al. [6] are bracketed by these two Sturmian results, as are the experimental results of Ford and Thomas and, when extrapolated from 80 keV, probably the experimental results of Lenormand [30] and Brower and Pipkin [31] as well. At 50 keV, there is a factor of 2.5 spread among the present coupled-state results and those of Jain, Lin, and Fritsch and Slim et al., reflecting basis sensitivity much as for the $3p$ state, with the present result again being between the other two. The three sets of experimental results lie within the spread of the theoretical results at this energy.

D. Capture into the $2pm$, $3pm$, and $3dm$ magnetic sublevels

Normalized Sturmian cross sections for electron transfer into the $2pm$, $3pm$, and $3dm$ magnetic sublevels are given in Table II. As is customary, the cross section for capture into a given nlm state has been normalized by dividing it by the s-state cross section for the same value of n.

It is seen that at the higher energies, the normalized nlm cross sections do not depend much on n: those for the $2pm$ and $3pm$ states are the same to within 25% for energies of at least 100 keV. At 50 keV, on the other hand, the normalized $3p_0$ cross section exceeds that for the $2p_0$ state by a factor of 2.

The basis dependence of the normalized magnetic sublevel cross sections, which has not yet been discussed, is generally slight at 100 keV: The results in Table II indicate differences between 48- and 51-state cross sections of

TABLE II. Ratio of Sturmian cross section Q_{nlm}/Q_{ns} for electron transfer into the magnetic sublevel[a] nlm to that for transfer into the ns state in collisions between protons and ground-state helium atoms.

Proton energy (keV)	No. of basis functions[b]	State						
		$2p_0$	$3p_0$	$2p_1$	$3p_1$	$3d_0$	$3d_1$	$3d_2$
50	40	0.131	0.266	0.0513	0.0602	0.0362	0.0031	0.000 41
100	37	0.103	0.0790	0.0434	0.0447	0.0316	0.0027	0.000 54
100	48	0.0770	0.0776	0.0426	0.0460	0.0072	0.0019	0.000 49
100	51	0.0718	0.0897	0.0432	0.0467	0.0183	0.0017	0.000 47
200	48	0.103	0.118	0.0494	0.0545	0.0285	0.0020	0.000 52
200	41	0.209	0.248	0.0316	0.0338	0.0412	0.0021	0.000 22
200	46	0.209	0.257	0.0335	0.0383	0.0351	0.0018	0.000 21

[a]The ratios for $m > 0$ are for $\pm m$ combined.
[b]The basis functions are defined in Table I.

at most 14%, with the exception of the $3d_0$ cross section. The sensitivity of more than a factor of 2 for this state gives rise to the factor-of-2 sensitivity in the summed $3d$ cross section noted previously. With the exception of that for the $3d_1$ state, all the cross sections at 200 keV, particularly the $m = 0$ components for a given l, are significantly sensitive, giving rise to the sensitivity noted previously in the cross sections summed over m. (This sensitivity in the sums, however, is mitigated somewhat by opposite sensitivity for $m = 0$ and 1.)

There are two other sets of normalized coupled-state cross sections for the magnetic sublevels—those of Jain, Lin, and Fritsch [5] and Slim et al. [6]—and two sets of experimental results—those of Brower and Pipkin [31] and Ashburn et al. [34].

Consider first the results of Jain, Lin, and Fritsch for the $2pm$ and $3pm$ states at lower energies; these are the only results for both $n = 2$ and 3. Except for the $2p_0$ state at 50 keV, the agreement with the Sturmian results is within 25% for the $2p_0$ and $3p_0$ states. Differences for the $2p_1$ and $3p_1$ states are usually about a factor of 2, the Sturmian results being larger. (In this discussion for energies of 50–100 keV, their results for the $3p_0$ and $3p_1$ states have been extrapolated from 80 to 100 keV.)

All the normalized cross sections for the $3p_0$ and $3p_1$ states are shown in Fig. 10. For the $3p_0$ state, the trend of the cross sections is downward with increasing energy, except for an inflection in the coupled-state results of Slim et al. from 80 to 100 keV and a rise in the Sturmian results from 100 to 200 keV. However, since the $3p_0$ Sturmian results display a large sensitivity to ionization channels at 200 keV, it is not clear what significance can be attached to the apparent rise there. The results of Slim et al. show a large sensitivity to the inclusion of interatomic exchange, particularly at 50 keV. At this energy, there is also a large difference between the present results and those of Slim et al. without exchange; the sensitivities to basis and exchange are comparable here. Extrapolating the results of Jain, Lin, and Fritsch to 100 keV, all the coupled-state results without exchange agree

to within 20% there, whereas the exchange effect is larger. Roughly consistent with the coupled-state results, the experimental data do not favor any particular one.

The normalized $3p_1$ cross sections in Fig. 10 show much less dependence on energy than do the $3p_0$ cross sections; indeed, beyond 80 keV, the cross section is
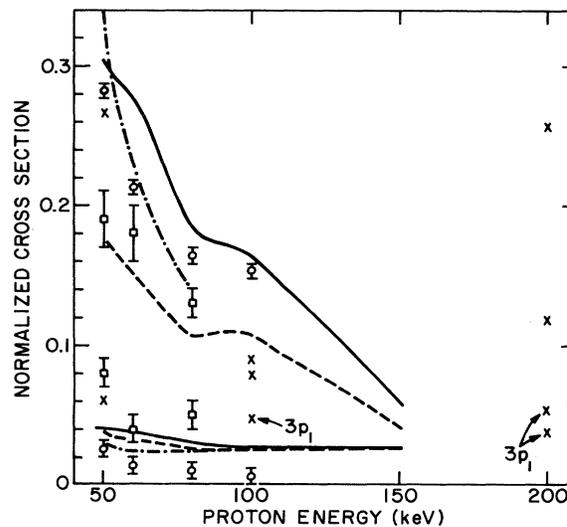

FIG. 10. Ratios Q_{3pm}/Q_{3s} of cross sections for electron transfer into the magnetic sublevels $3pm$ to that for transfer into the $3s$ state in collisions between protons and helium atoms. The upper sets of data are for $m = 0$. (The data for $m = 1$ are for ± 1 combined.) Coupled-state results: crosses, present 46–51-Sturmian (40-Sturmian at 50 keV); solid and dashed curves, 33-pseudostate with and without exchange, respectively, Slim et al. (Ref. [6]); dash-dotted curves, 19-state AO+, Jain, Lin, and Fritsch (Ref. [5]). Experimental results: open squares, Brower and Pipkin (Ref. [31]); open circles, Ashburn et al. (Ref. [34]).

mostly flat (or has a slight rise). The sensitivity to exchange is smaller than the sensitivity to basis. The results of Slim *et al.* with or without exchange and the results of Jain, Lin, and Fritsch generally lie between the two sets of experimental data, whereas the data of Brower and Pipkin seem to favor the present result, which is about 50% to a factor of 2 above the other coupled-state results.

Consider now the normalized cross sections for the $3d_0$ state, shown in Fig. 11 along with those for the $3d_1$ state. The $3d_0$ cross sections are somewhat similar to those for the $3p_0$ state in that the theoretical cross sections display a rapid falloff with energy at lower energies. At higher energies above about 100 keV, the dependence is less clear; the Sturmian cross section may rise, but it is again sensitive to the inclusion of ionization channels. The sensitivity to exchange displayed in the results of Slim *et al.* is only 25%, less than for the $3p_0$ state. The experimental data have larger uncertainties than for the $3p_0$ state, and do not differ greatly. Taken together, they do not favor any particular one of the coupled-state results over the full energy range.
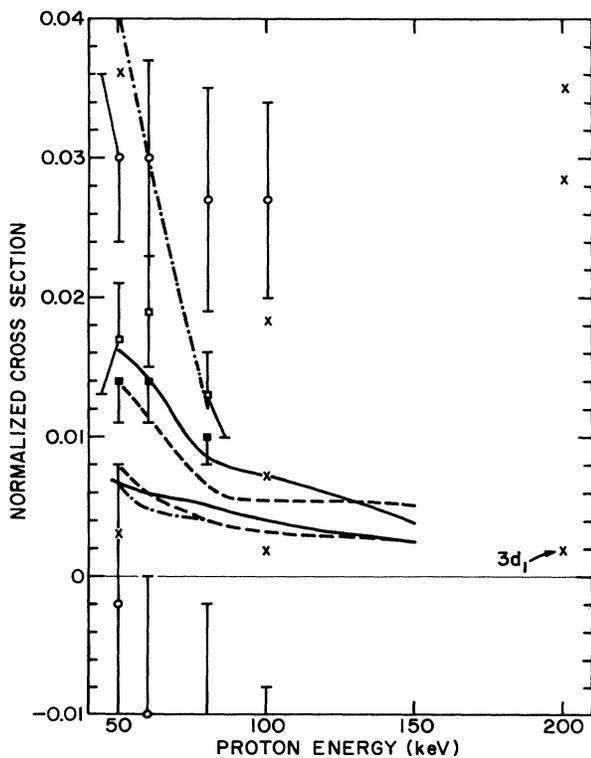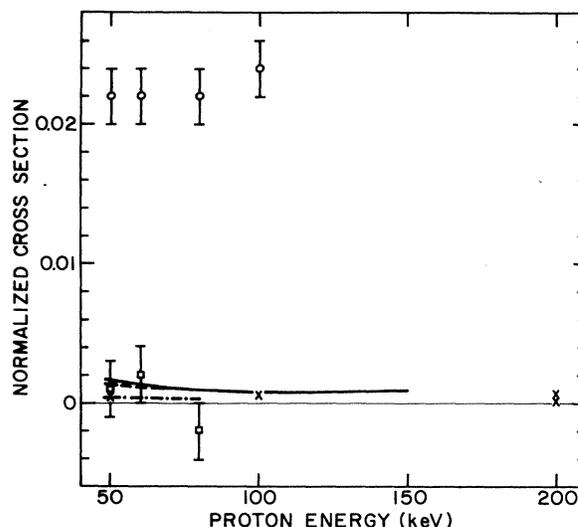
FIG. 12. Ratios Q_{3d2}/Q_{3s} of cross sections for electron transfer into the magnetic sublevel $3d_2$ to that for transfer into the $3s$ state in collisions between protons and helium atoms. The notation is as in Fig. 10.

FIG. 11. Ratios Q_{3dm}/Q_{3s} of cross sections for electron transfer into the magnetic sublevels $3dm$, $m=0,1$, to that for transfer into the $3s$ state in collisions between protons and helium atoms. The notation is as in Fig. 10, except that the solid squares are the experimental data of Brower and Pipkin for $m=1$.

The normalized $3d_1$ cross section in Fig. 11 has a smaller energy dependence, not unlike that for the $3p_1$ state. The dependence on exchange is not more than about 25%. The present result is below the other coupled-state results by 50% to a factor of 2, whereas for the analogous $3p_1$ state it was noted to be higher by 50% to a factor of 2. All the coupled-state results generally lie between the two sets of experimental results.

Consider finally the normalized $3d_2$ cross section shown in Fig. 12. All the results agree in having little or no energy dependence. The effect of exchange is small, at most 20%. The present result agrees more closely with that of Jain, Lin, and Fritsch than Slim *et al.* at 50 keV. The experimental data of Brower and Pipkin are generally consistent with all the coupled-state results, whereas the data of Ashburn *et al.* are at least an order of magnitude higher.

E. $\langle \mathbf{D} \rangle_z$ and $\langle \mathbf{L} \times \mathbf{A} \rangle_{s,z}$

The Sturmian values of the z component of the average electric dipole moment $\langle \mathbf{D} \rangle$ and of the symmetrized cross product $\langle \mathbf{L} \times \mathbf{A} \rangle_s$ between the angular momentum and the Runge-Lenz vector are given in Table III for capture into the $n=2,3$ levels of hydrogen. For either value of n, $\langle \mathbf{D} \rangle_z$ and $\langle \mathbf{L} \times \mathbf{A} \rangle_{s,z}$ depend on the real and imaginary parts, respectively, of the s,lm off-diagonal density matrix elements for $m \leq 1$.

Consider first the dependence of each quantity on principal quantum number n. It is seen in Table III that for

TABLE III. Sturmian values of the z component of the average electric dipole moment $\langle D \rangle$ and of the symmetrized cross product $\langle L \times A \rangle_s$ between the angular momentum and the Runge-Lenz vector for capture into the $n = 2$ and 3 levels of hydrogen in proton-helium collisions.

Proton energy (keV)	No. of basis functions[a]	$\langle D \rangle_z$		$\langle L \times A \rangle_{s,z}$	
		$n = 2$	$n = 3$	$n = 2$	$n = 3$
50	40	0.986	3.22	0.0789	0.588
100	37	0.932	2.13	−0.487	−0.674
100	48	0.750	2.06	−0.318	−0.369
100	51	0.640	2.30	−0.312	−0.283
200	48	0.573	1.63	−0.472	−0.64
200	41	1.60	3.59	−0.385	−0.51
200	46	1.55	3.69	−0.407	−0.55

[a]The basis functions are defined in Table I.

either value of n, the dipole moment decreases as the energy increases from 50 to 100 keV, and results at 100 keV are not strongly basis sensitive. At 200 keV, there is a strong basis sensitivity; the results do, however, indicate that the dipole moment either rises for both n or remains approximately constant for both n over energies from 100 to 200 keV. The only other coupled-state results available for both n are those of Jain, Lin, and Fritsch up to 100 keV. Their results also decline with energy for either n, but more steeply.

The basis sensitivity of $\langle L \times A \rangle_{s,z}$ is less than for $\langle D \rangle_z$, so its energy dependence can be established over the full range 50–200 keV. For both values of n, $\langle L \times A \rangle_{s,z}$ decreases with increasing energy. The results of Jain, Lin, and Fritsch in the range 50–100 keV also decrease for both values of n, but the details differ.

For the $n = 3$ level, Slim et al. have, in addition to Jain, Lin, and Fritsch, reported coupled-state values of $\langle D \rangle_z$ and $\langle L \times A \rangle_{s,z}$. The only experimental results are those of Ashburn et al. Consider first $\langle D \rangle_z$, shown in Fig. 13. It is seen that all the results generally decline with energy, the present results at the same rate as the experimental results of Ashburn et al. up to 100 keV.

However, these experimental results are 30% higher. The results of Slim et al. indicate that the effect of interatomic exchange decreases from 50% to 50 keV to about 20% at energies 100–150 keV. At 100 keV, but not 50 keV, the basis sensitivity (as reflected in the spread of the coupled-state results without exchange) exceeds this sensitivity to exchange. At higher energies, the present results do not differ greatly from the continuum-distorted-wave post-collision-interaction (CDW-PCI) results [35] of Burgdörfer and Dubé (not shown); the difference between the lower Sturmian value at 200 keV and the CDW-PCI value is 35%.

Consider finally $\langle L \times A \rangle_{s,z}$ for the $n = 3$ level, shown in Fig. 14. Over the range 50–100 keV, the experimental and all coupled-state results generally decrease with energy. Beyond 100 keV, the results of Slim et al. are constant or show a slight rise, whereas the Sturmian results and the CDW-PCI results [35] of Burgdörfer and Dubé (not shown) continue to decrease somewhat. At both 50 and 100 keV, the difference among all the coupled-state results without exchange exceeds the sensitivity to exchange.

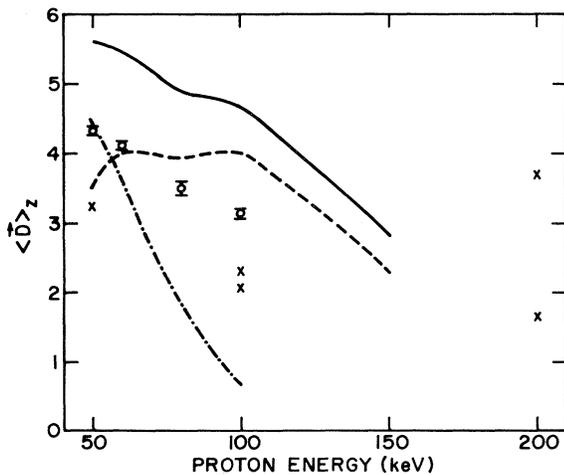*Note added in proof.* Experimental results in addition

FIG. 13. Values of the z component of the average electric dipole moment $\langle D \rangle$ for electron transfer into the $n = 3$ level of hydrogen in proton-helium collisions. The notation is as in Fig. 10.
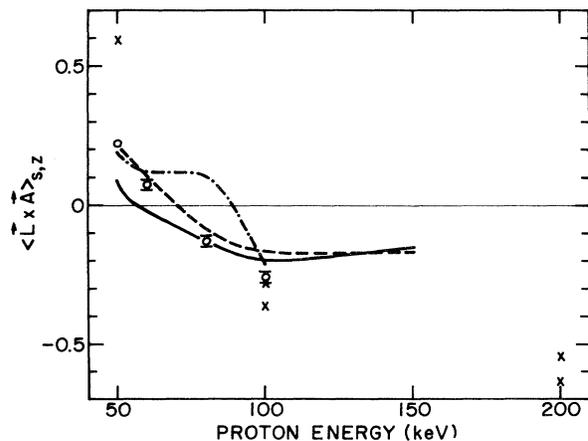

FIG. 14. Values of the z component of the symmetrized cross product $\langle L \times A \rangle_s$ between the angular momentum and the Runge-Lenz vector for electron transfer into the $n = 3$ level of hydrogen in proton-helium collisions. The notation is as in Fig. 10.

to those cited in the text have recently been reported, and one earlier experiment was overlooked. Cline et al. [Phys. Rev. A **43**, 1611 (1991)] have reported cross sections for electron capture into the $3s$, $3p$, and $3d$ states of hydrogen in proton-helium collisions up to 100 keV. Their cross sections were normalized to the $3s$ cross section of Brower and Pipkin (Ref. [31]) at 60 keV. For the energies of at least 50 keV of interest here, their results agree closely with those of Brower and Pipkin for the $3s$ and $3p$ states and Hughes et al. (Ref. [28]) for the $3d$ state; the overall comparison in the text between theory and experiment is not altered. Hippler et al. [Z. Phys. D **18**, 61 (1991)] have reported cross sections for capture into the $2p$ state for proton energies up to 300 keV. These results agree well with the Sturmian results at energies up to 100 keV, but at higher energies decrease more rapidly with energy; however, the basis sensitivity of the small Sturmian cross sections was noted to be large.

The quantities $\langle D \rangle_z$ and $\langle L \times A \rangle_{s,z}$ for the $n = 2$ level have been measured by three groups: Hippler et al. [Phys. Rev. A **43**, 2587 (1991)] at energies up to 25 keV, Cline et al. [Bull. Am. Phys. Soc. **36**, 1309 (1991)] at en-

ergies up to 100 keV, and De Serio et al. [Phys. Rev. A **37**, 4111 (1988)] at higher energies. The experimental results of Hippler et al., which are below the energy range of the present study, do, however, tie into the results of Cline et al. at 25 keV. The Sturmian results for $\langle D \rangle_z$ and $\langle L \times A \rangle_{s,z}$ genreally agree with the results of Cline et al. at lower energies and are consistent with those of De Serio et al. at higher energies except that at the lower energies the Sturmian results for $\langle D \rangle_z$ [as well as the coupled-state results of Jain, C. D. Lin, and Fritsch] (Ref. [5]) decline with energy in contrast to those of Cline et al.

*Permanent address.

[1] T. A. Green, H. E. Stanley, and Y.-C. Chiang, Helv. Phys. Acta **38**, 109 (1965).

[2] B. H. Bransden and L. T. Sin Fai Lam, Proc. Phys. Soc. London **87**, 653 (1966).

[3] L. T. Sin Fai Lam, Proc. Phys. Soc. London **92**, 67 (1967).

[4] T. G. Winter and C. C. Lin, Phys. Rev. A **10**, 2141 (1974).

[5] A. Jain, C. D. Lin, and W. Fritsch, Phys. Rev. A **36**, 2041 (1987).

[6] H. A. Slim, E. L. Heck, B. H. Bransden, and D. R. Flower, J. Phys. B **23**, L611 (1990).

[7] T. G. Winter, Phys. Rev. A **25**, 697 (1982). In Eq. (33) of this paper, the l subscript on $\mathcal{Y}$ should be L, and Eqs. (46) and (47) should contain a factor $(-1)^{m+m_1+m'+m'_1}$.

[8] T. G. Winter, Phys. Rev. A **33**, 3842 (1986).

[9] T. G. Winter, Phys. Rev. A **35**, 3799 (1987).

[10] C. D. Stodden, H. J. Monkhorst, K. Szalewicz, and T. G. Winter, Phys. Rev. A **41**, 1281 (1990).

[11] R. Shakeshaft, Phys. Rev. A **18**, 1930 (1978).

[12] D. F. Gallaher and L. Wilets, Phys. Rev. **169**, 139 (1968).

[13] T. G. Winter, Phys. Rev. A **43**, 4727 (1991).

[14] J. R. Winter (private communication).

[15] Seven $(n_1 s n_2 s)$ ^1S helium-centered functions (with $n_1 \leq 2$, $n_2 \leq 4$, and $n_1 \leq n_2$) and eleven $2p_{0,1}, \ldots, 5p_{0,1}, 3d_{0,1,2}$ Sturmian functions centered on the proton, with the He^+ ion in the ground state.

[16] These tests have been carried out using the same He-centered functions as for the s Sturmian tests, plus a fixed number (11) of s Sturmian functions centered on the proton as well as $3d_{0,1,2}$ Sturmian functions except for $n_{p \, max} \leq 2$ for which $3d_{0,1,2}$ Sturmian functions are omitted.

[17] The bases used in this test include also the 30 proton-centered Sturmian functions up to $13s$, $8p_{0,1}$, and $3d_{0,1,2}$.

[18] The bases used in this test include also the ten $n_1 s n_2 s$ and $n'_1 p n'_2 p$ ^1S He-centered functions with $n_1 \leq 2$, $n_2 \leq 4$, $n_1 \leq n_2$, $n'_1 \leq 3$, $n'_2 \leq 3$, and $n'_1 \leq n'_2$ and the 24 proton-centered Sturmian functions up to $11s$, $6p_{0,1}$, and $3d_{0,1,2}$.

[19] The bases also include seven ns He-centered Sturmian functions as well as the same 24 proton-centered Sturmian functions as for the two-electron test.

[20] The fixed part of the bases now consists of only the $1s, 2p_{0,1}$ proton-centered states and no ns He-centered states other than the initial state.

[21] The bases used in these tests include also seven $n_1 s n_2 s$ ^1S functions centered on helium, and 24 Sturmian functions up to $11s$, $6p_{0,1}$, and $3d_{0,1,2}$ centered on the proton.

[22] M. B. Shah and H. B. Gilbody, J. Phys. B **18**, 899 (1985).

[23] This Sturmian contribution has been used to add on an excited-state contribution to the coupled-state results of Winter and Lin (Ref. [4]) and Jain, Lin, and Fritsch (Ref. [5]) for energies of at least 50 keV; below 50 keV, that contribution has been estimated to be 20%.

[24] C. F. Barnett and H. K. Reynolds, Phys. Rev. **109**, 355 (1958).

[25] L. H. Toburen, M. Y. Nakai, and R. A. Langley, Phys. Rev. **171**, 114 (1968).

[26] R. J. Conrads, T. W. Nichols, J. C. Ford, and E. W. Thomas, Phys. Rev. A **7**, 1928 (1973).

[27] R. H. Hughes, E. D. Stokes, S.-S. Choe, and T. J. King, Phys. Rev. A **4**, 1453 (1971).

[28] R. H. Hughes, C. A. Stigers, B. M. Doughty, and E. D. Stokes, Phys. Rev. A **1**, 1424 (1970).

[29] E. P. Andreev, V. A. Ankudinov, and S. V. Bobashev, Zh. Eksp. Teor. Fiz. **50**, 565 (1966) [Sov. Phys.—JETP **23**, 375 (1966)].

[30] J. Lenormand, J. Phys. (Paris) **37**, 699 (1976).

[31] M. C. Brower and F. M. Pipkin, Phys. Rev. A **39**, 3323 (1989).

[32] J. C. Ford and E. W. Thomas, Phys. Rev. A **5**, 1964 (1972).

[33] F. J. de Heer, J. van Eck, and J. Kistemaker, *Proceedings of the Sixth International Conference on Ionization Phenomena in Gases* (Serma, Paris, 1963), Vol. 1, p. 73.

[34] J. R. Ashburn, R. A. Cline, P. J. M. van der Burgt, W. B. Westerveld, and J. S. Risley, Phys. Rev. A **41**, 2407 (1990).

[35] J. Burgdörfer and L. J. Dubé, Phys. Rev. Lett. **52**, 2225 (1984).